catalysts

MDPI

Article

Efficient Production of Medium-Chain Structured Phospholipids over Mesoporous Organosulfonic Acid-Functionalized SBA-15 Catalysts

Jianghua Zhang [1,2], Shasha Yang [1], Weijie Cai [1], Fawen Yin [2], Jin Jia [1], Dayong Zhou [2,*] and Beiwei Zhu [2]

1 School of Light Industry and Chemical Engineering, Dalian Polytechnic University, Dalian 116034, China; zhang_jh@dlpu.edu.cn (J.Z.); YangShasha1202@163.com (S.Y.); caiwj@dlpu.edu.cn (W.C.); jiajin19931122@163.com (J.J.)

2 National Engineering Research Center of Seafood, Dalian Polytechnic University, Dalian 116034, China; yinfawen1988@126.com (F.Y.); zhubeiwei@163.com (B.Z.)

* Correspondence: zdyzf1@163.com; Tel.: +86-411-86323262

Received: 13 August 2019; Accepted: 11 September 2019; Published: 13 September 2019

Abstract: It is highly desirable that efficient recoverable heterogeneous catalysts should be developed to replace the costly biocatalysts used in producing structured phospholipids (SPLs) with medium-chain fatty acids (MCFAs). Thus, mesoporous propyl and phenyl sulfonic acid-functionalized SBA-15 materials synthesized via surface modification methods were investigated for the soybean lecithin interesterification with methyl caprate or caprylate. The physicochemical properties of the synthesized solid acids were deeply studied by small-angle X-ray diffraction, scanning electron microscopy, transmission electron microscopy, Fourier transform infrared and pyridine adsorption, etc. to build the possible structure–performance relationships. The results revealed that amounts of organosulfonic acid groups were successfully grafted onto the SBA-15 support, and most of the surface acid sites contained in the as-prepared organic–inorganic hybrid samples were assigned as strong Brönsted acid sites. Notably, the functionalized SBA-15 materials exhibited promising catalytic behaviors in producing MCFA-enriched SPLs under mild conditions (40 °C, 6 h) when compared with commercial Amberlyst-15 and typical phospholipases or lipases, mostly due to their high surface area, ordered structure and adequate Brönsted acid sites. Besides, the as-prepared materials could be easily recycled five times without obvious deactivation. This work might shed light on alternative catalysts for SPL production instead of the costly enzymes.

Keywords: structured phospholipid; medium-chain fatty acid; heterogeneous catalyst; interesterification; lecithin

1. Introduction

At present, great efforts have been devoted to the catalytic production of structured lipids (SLs) from natural vegetable oils and/or phospholipids (PLs) to meet the increasing demands for high-valued chemicals, pharmaceuticals and nutraceuticals, etc. [1–4]. In particular, structured phospholipids (SPLs), known as efficient emulsifiers considering their surfactant properties, have achieved extensive attention owing to their versatile applications in fine chemical, pharmaceutical, cosmetic and food industries, etc. [5,6]. Among these, medium-chain SPLs were generally produced by incorporating medium-chain fatty acids (MCFAs) with 6 to 10 carbon-chain lengths into native long-chain PLs to enhance their original physicochemical characteristics, functional attributes and nutritional effects, and meanwhile to improve the emulsification activity and heat stability [5,7]. Furthermore, MCFA-enriched SPLs could be utilized as healthy functional lipids for medical and food applications due to their lower

caloric values and fat depositions, etc. Notably, the SPLs with MCFAs could also be considered as a kind of accessible energy source for those patients with absorption problems because of the much greater fatty acid (FA) bioavailabilities in the PL forms [8,9]. Accordingly, the increasing requirements for MCFA-enriched SPLs might greatly stimulate their large-scale production, which could present a remarkable challenge for academic research and industry.

Recently, the MCFA-enriched SPLs have been mostly produced by the interesterification reactions of PLs, where the FAs in native PLs are replaced by the desirable MCFAs. Nevertheless, all these processes were carried out by using expensive enzyme catalysts and displayed several drawbacks, such as the lack of operational stability, costly separation and poor recyclability, etc. [10–12]. Otherwise, to the best of our knowledge, no heterogeneous catalysts, especially for solid acids, have been employed in the modification of natural PLs through interesterification reactions. Alternatively, from the standpoint of cleaner production and sustainable development [13,14], it is extremely important to develop heterogeneous solid acid catalysts with high efficiency and attractive stability for the production of MCFA-enriched SPLs from natural PL feedstocks by interesterification reactions.

Over the past few years, extensive research has focused on heterogeneous acid catalysts utilized in interesterification reactions, like graphene-based solid acids [14], biomass-based sulfated carbon [15], commercial Amberlyst-15 [16], sulfated zirconia [17], sulfated zirconia-silica [18] and functionalized SBA-15 [19], etc. Among these various candidates, SBA-15 type solid acids were perceived as one of the most engaging solid acid catalysts due to their excellent structural properties, including the relatively tunable pore size, high surface area and good stability together with the efficient, environmentally benign and convenient natures [19,20]. More importantly, these SBA-15 materials attracted considerable attention because of their facile modification with numerous catalytically active acid groups. In general, it was accepted that amounts of active Brönsted acid sites in catalysts would be favorable for the interesterification reactions [21]. Hence, it could be an active research topic to exploit the functionalized SBA-15 materials with abundant Brönsted acid sites in order to develop highly efficient catalysts for the production of MCFA-enriched SPLs via PL interesterification.

On the other hand, different modification methods have been used to prepare various SBA-15 type mesoporous materials with prominent structural features and catalytic performances. Noticeably, extensive interest has been centered on the introduction of organosulfonic acid groups into the mesostructure of reference SBA-15 to enhance its Brönsted acid sites [22]. Generally, the organosulfonic acid moieties were covalently bound onto the surfaces of SBA-15 silica. Consequently, the inorganic–organic hybrid mesoporous materials with multiple strong Brönsted acid sites were successfully achieved. And the resultant solid acids could possess abundant reactive and mechanical properties attributed to the intercalation of organic species into inorganic solids [23]. Furthermore, the catalytic performances of the inorganic–organic hybrid materials could be well maintained because the leaching of active organosulfonic acid groups would be avoided during the reaction processes, mostly owing to the existence of covalent bonds [22]. Therefore, the organosulfonic acid-modified SBA-15 catalysts might be the appropriate candidates for the production of MCFA-enriched SPLs from native PLs under mild conditions with high MCFA incorporations.

Inspired by the present work, two mesoporous organosulfonic acid-functionalized SBA-15 materials are prepared by surface modification and selected as heterogeneous catalysts for the production of MCFA-enriched SPLs by the interesterification of soybean lecithin (SL) with methyl caprate or caprylate (Scheme 1). The acidities and structural properties of the catalysts are studied in detail by a series of characterization techniques, such as N_2 adsorption–desorption, small-angle X-ray diffraction (XRD), scanning electron microscopy (SEM), transmission electron microscopy (TEM), Fourier transform infrared (FT-IR) and Pyridine-FT-IR (Py-FT-IR), etc., to build the possible structure–performance relationships. The interesterification parameters are optimized based on the incorporations of MCFAs into SLs and the catalyst reusability is investigated as well. Compared with the commercial Amberlyst-15, the as-prepared SBA-15 solid acids exhibit promising catalytic performances and great potential for the efficient production of MCFA-enriched SPLs from natural PLs.

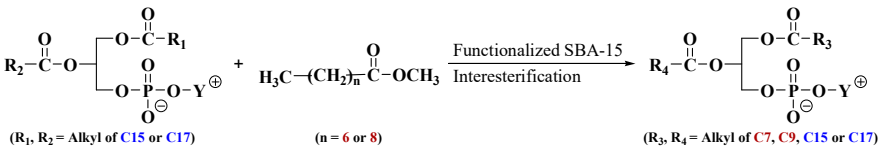

Scheme 1. Catalytic synthesis of MCFA-enriched SPLs by SL interesterification.

2. Results and Discussion

2.1. Catalyst Characterization

The physicochemical features of modified SBA-15 materials and reference SBA-15 were investigated via various characterization techniques. Firstly, the textural properties of the samples were studied by using N_2 adsorption–desorption isotherms and pore-size distributions, as illustrated in Figure 1. Notably, all the samples exhibited type IV patterns based on IUPAC classifications, with sharp capillary condensation steps in the region of $0.4 < p/p_0 < 0.8$ and typically steep H1 hysteresis loops [24]. The results implied the existence of ordered mesoporous channels in the synthesized samples and further confirmed the retainment of the intact mesoporous structure of SBA-15 after surface modification [25]. Furthermore, the mean pore-size distributions calculated by the Barrett–Joyner–Halenda (BJH) method (Figure 1B) elucidated the narrow pore-size ranges centered at ca. 5.03–7.23 nm supporting the ordered mesostructure natures of the investigated SBA-15 samples [25]. On the other hand, the specific surface areas of the meso-Pr-SO_3H-SBA-15 and meso-Ph-SO_3H-SBA-15 were calculated to be around 558.1 and 582.3 m^2/g, respectively, by the Brunauer–Emmett–Teller (BET) method. Correspondingly, the pore volumes of the two samples were ca. 0.89 and 0.88 cm^3/g, respectively. Remarkable decreases were observed when compared with the values of as-prepared SBA-15 support (ca. 622.3 m^2/g and 1.02 cm^3/g). It indicated that numerous functionalized groups were incorporated into the SBA-15 mesoporous structure and further occupied some parts of the channel spaces, as reported in the previous publication [26]. Therefore, the above-mentioned results suggested that the ordered mesoporous structure of original SBA-15 was still retained in the modified SBA-15 materials with high BET surface areas and pore volumes even after the organofunctionalization, which was favorable for the SL interesterification.

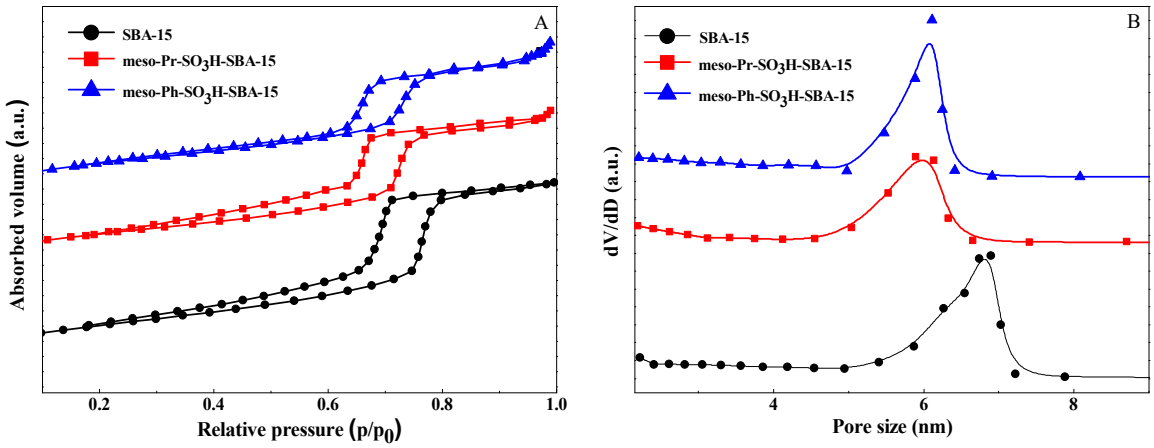

Figure 1. Nitrogen adsorption–desorption isotherms (**A**) and pore-size distributions (**B**) of SBA-15, mesoporous propyl sulfonic acid-functionalized SBA-15 (meso-Pr-SO_3H-SBA-15) and mesoporous phenyl sulfonic acid-functionalized SBA-15 (meso-Ph-SO_3H-SBA-15) samples.

The integrity of the structure of the SBA-15 catalyst and compared SBA-15 support was illustrated by the high-angle XRD in the 2theta range of 10°–80°. The patterns of the synthesized SBA-15 samples are displayed in Figure 2A. It could be clearly observed that each SBA-15 sample exhibited only a

broad peak in the 2theta range of 10°–40°. This phenomenon was assigned to the amorphous nature of the SBA-15 sample in good agreement with the previous report [20]. As for the mesostructure of the SBA-15 sample, it could be verified by the low-angle XRD in the 2theta range of 0°–6°. Figure 2B showed the patterns of the as-prepared samples. Obviously, all the SBA-15, meso-Pr-SO_3H-SBA-15 and meso-Ph-SO_3H-SBA-15 materials presented three characteristic XRD diffraction peaks centered at ca. 0.90°, 1.52° and 1.75°. In general, the three typical peaks were indexable as reflections of (100), (110) and (200) planes of ordered mesoporous SBA-15 type material associated with a two-dimensional (2D) hexagonal symmetry (P6mm), which were in accordance with those of other functionalized SBA-15 materials prepared using similar strategies. [27,28]. Accordingly, the low-angle XRD results implied that the 2D hexagonal mesostructure of SBA-15 silica was virtually maintained in the functionalized SBA-15 samples after undergoing the organic sulfonation processes, which was consistent with the N_2 adsorption–desorption isotherms [29].

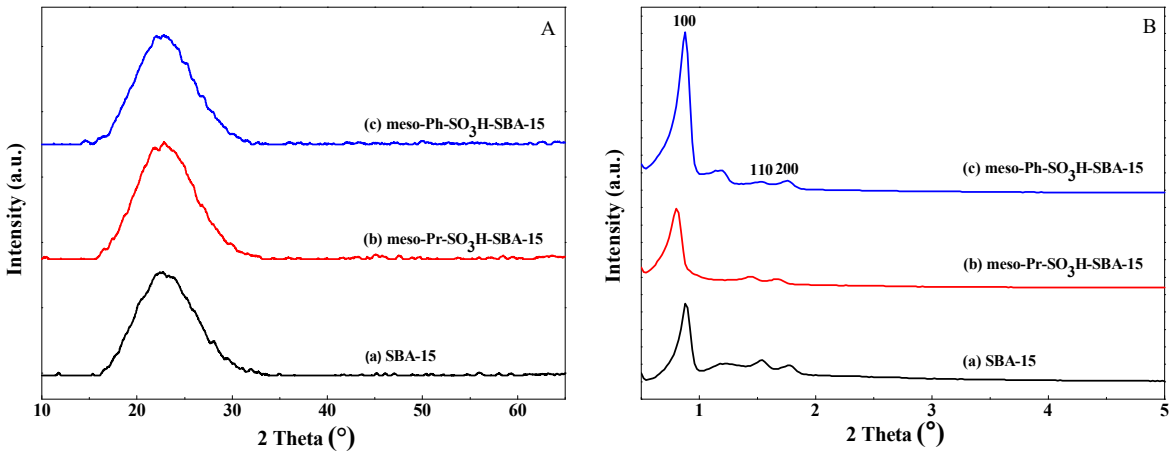

Figure 2. The high-angle (**A**) and low-angle (**B**) XRD patterns of SBA-15 and two modified SBA-15 samples.

The surface morphologies and microstructures of the obtained SBA-15 materials were studied by using SEM and TEM techniques. As illustrated in Figure 3A–C, a great number of well-defined wheat-like particles, with average sizes of around 0.5 μm, appeared in the meso-Pr-SO_3H-SBA-15 and meso-Ph-SO_3H-SBA-15 samples similar to the parent SBA-15. Meanwhile, the two modified SBA-15 materials exhibited rougher surfaces and/or denser structures than the SBA-15 support owing to the surface functionalization, which was in good line with the previous literature [26]. Besides, Figure 3D–F showed the TEM images of the three samples. It was obvious that both the modified SBA-15 materials presented one-dimensional and well-ordered arrays with ca. 6 nm wide channels similar to the original SBA-15 specimen. Thus, the SEM and TEM results indicated that the organosulfonic acid-functionalized SBA-15 materials essentially retained the ordered mesoporous silica SBA-15 framework after the surface grafting with organic moieties, which would enhance catalytic acid site accessibility. Furthermore, Figure 4 illustrates the carbon, oxygen, silicon and sulfur elemental mappings and energy-dispersive X-ray spectroscopy (EDX) images from randomly selected regions (Figure 4A,a) of the organofunctionalized SBA-15 materials. It was observed clearly that sulfur was successfully introduced and uniformly dispersed on the catalyst surfaces compared to the reference SBA-15, suggesting the presence of highly distributed organosulfonic acid groups [30]. Thus, it was indicated that high densities of organosulfonic acid groups were achieved in thus-synthesized solid acids by sulfonate-functionalization without damaging the order structure of the SBA-15 support, which would have a positive effect on the SL interesterification.

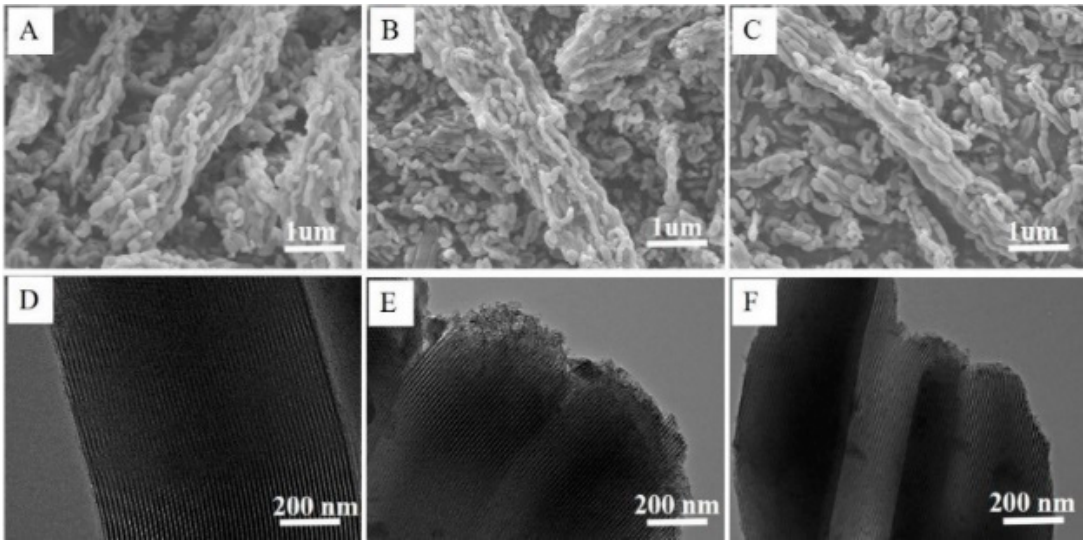

Figure 3. SEM and TEM images of SBA-15 (**A**,**D**), meso-Pr-SO_3H-SBA-15 (**B**,**E**) and meso-Ph-SO_3H-SBA-15 (**C**,**F**) samples.

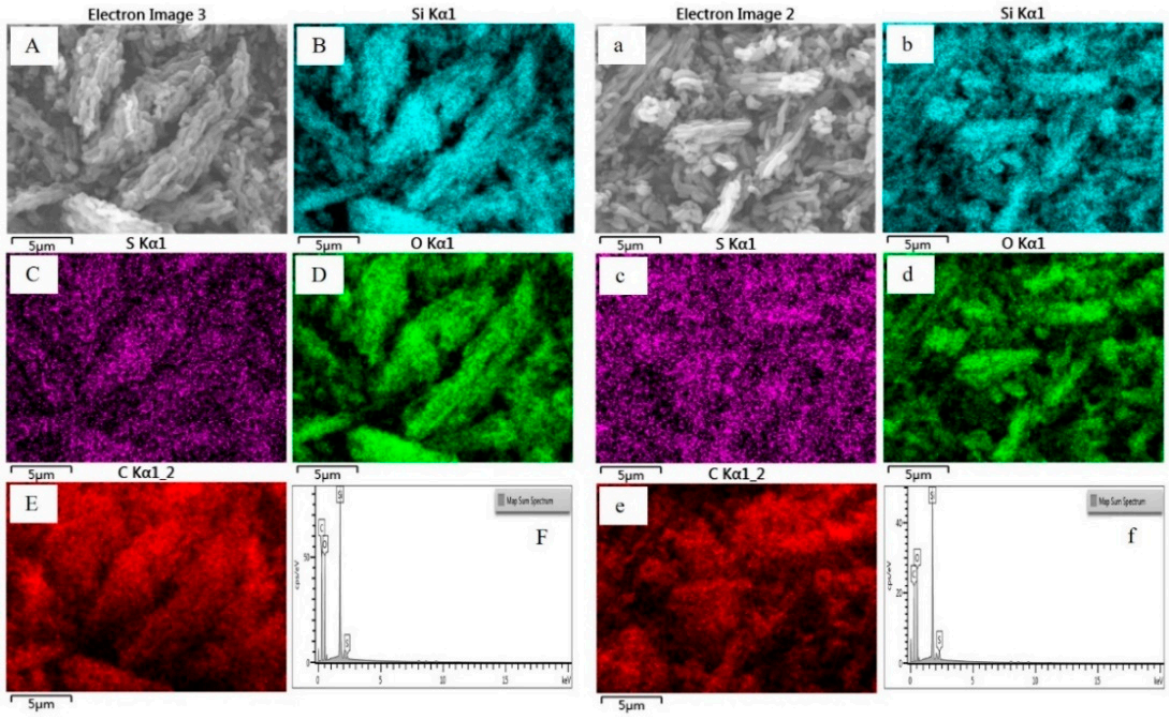

Figure 4. SEM images (**A** and **a**), silicon (**B** and **b**), sulfur (**C** and **c**), oxygen (**D** and **d**), carbon (**E** and **e**) elemental mappings and EDX analyses (**F** and **f**) of meso-Pr-SO_3H-SBA-15 (**A**–**F**) and meso-Ph-SO_3H-SBA-15 (**a**–**f**) samples.

In order to further confirm the surface functional groups on the investigated SBA-15 samples, FT-IR analyses were performed and the spectra were shown in Figure 5A. Firstly, the successful grafting of sulfonic groups onto the silica framework was evidenced by curves (b) and (c). Two characteristic bonds observed at around 1070 and 650 cm^{-1} were identified as O=S=O and C-S stretching vibrations, respectively. Besides, the absorption peaks centered at ca. 3430 and 1630 cm^{-1} were attributed to S-OH stretching vibrations in -SO_3H groups [31]. These FT-IR results suggested that the -SO_3H groups were anchored onto the surfaces of as-synthesized modified SBA-15 materials, which were always viewed as the active Brönsted acid sites of the catalyst [32]. In addition, the bands observed at about 1080,

780 and 450 cm^{-1} from the three curves corresponded to the Si-O-Si stretching and bending vibrations, suggesting the presence of SBA-15 structure. And the FT-IR peaks located at ca. 3400 and 960 cm^{-1} were assigned to the surface -OH stretching mode and the Si-OH bending vibration, supporting the aforementioned view [26]. Otherwise, the existence of propyl groups was confirmed by the bands at about 2930 and 2854 cm^{-1} in curve (b), ascribed to the C-H stretching vibration of methylene [33]. The peaks at ca. 1510, 1430 and 550 cm^{-1} in curve (c) were correspondingly attributed to the stretching vibrations of phenyl groups [34]. Based on all the FT-IR analyses, it was elucidated that propyl and phenyl groups, respectively, existed in the meso-Pr-SO_3H-SBA-15 and meso-Ph-SO_3H-SBA-15 samples with multiple Brönsted acid sites.

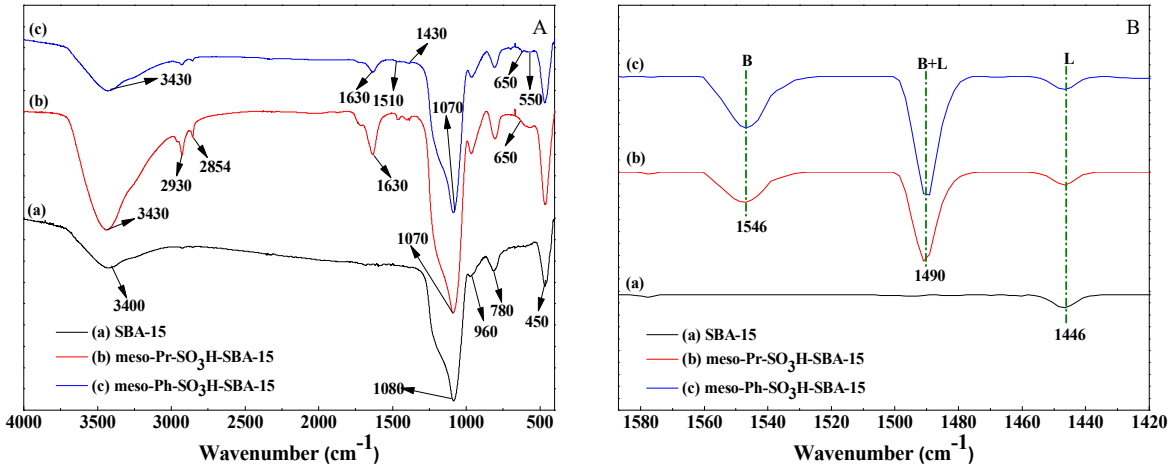

Figure 5. FT-IR spectra (**A**) and Py-FT-IR spectra (**B**) of SBA-15 (a), meso-Pr-SO_3H-SBA-15 (b) and meso-Ph-SO_3H-SBA-15 (c) samples.

It is well accepted that surface acid property is one of the key factors for the catalytic interesterification reactions of solid acids. In order to clarify the types of acid sites as well as their ratios on the catalyst surfaces, the corresponding Py-FT-IR spectra were collected and are depicted in Figure 5B. Three characteristic absorption bands at about 1546, 1490 and 1446 cm^{-1} confirmed the presence of Brönsted acid sites assignable to the N-H bending of the pyridinium ion, the mixture of Brönsted and Lewis acid sites and Lewis acid sites ascribed to pyridine coordination [35,36]. Obviously, the results revealed the coexistence of Brönsted and Lewis acid sites in the modified SBA-15 catalyst. In addition, it is notable that the relative intensities of the characteristic peaks are consistent with the acid site quantities. Correspondingly, the ratios of Brönsted acid sites to Lewis acid sites were calculated to be 7.5 (meso-Ph-SO_3H-SBA-15) and 5.2 (meso-Pr-SO_3H-SBA-15), respectively. The results indicated that most of the surface acid sites on the two SBA-15 solid acids (ca. 86% for meso-Ph-SO_3H-SBA-15 and ca. 79% for meso-Pr-SO_3H-SBA-15) were attributed to strong Brönsted acid sites. To further quantify the acid densities of Brönsted acid sites in the modified SBA-15 samples, acid-base titrations were conducted. Consequently, the values were measured to be 0.93 and 0.85 mmol/g for meso-Ph-SO_3H-SBA-15 and meso-Pr-SO_3H-SBA-15 materials, suggesting that both of the investigated samples belonged to strong solid acids. By contrast, it was determined that the meso-Ph-SO_3H-SBA-15 sample contained the larger acid site quantities, mostly due to the more electron withdrawing environments of its sulfonic acid sites, which would lead to the higher reaction performances in interesterifications. As for reference SBA-15, no peak at ca. 1546 cm^{-1} was observed in curve (a), meaning hardly any Brönsted acid sites existed in this support, which was verified by the titration result. Noticeably, many recent studies have reported that abundant Brönsted acid sites on solid acids could be responsible for the high interesterification activities of these catalysts [37,38]. Therefore, numerous Brönsted acid sites on the organosulfonic acid-modified SBA-15 silica could efficiently promote the SL interesterification under mild conditions.

2.2. Catalytic Production of SPLs with MCFAs

The organosulfonic acid-modified SBA-15 might be a more promising catalyst in the interesterification reactions based on the reasonable surface acid property. Hence, thus-synthesized SBA-15 solid acids were selected as potential catalysts for the efficient production of SPLs with MCFAs in this work. According to the results of initial blank tests, it was expected that no detectable MCFAs would be observed. Similarly, the reference SBA-15 displayed no considerable catalytic performances with the detection of trace amounts of MCFAs, which was in good line with the discussion of pyridine adsorption results (Figure 5B). In contrast, the additions of SBA-15 solid acids remarkably improved the capric acid (C10:0) incorporations (ca. 14.66 ± 0.57% for meso-Ph-SO_3H-SBA-15 and ca. 12.95 ± 0.64% for meso-Pr-SO_3H-SBA-15) and the caprylic acid (C8:0) incorporations (ca. 12.85 ± 0.33% for meso-Ph-SO_3H-SBA-15 and ca. 9.36 ± 0.52% for meso-Pr-SO_3H-SBA-15) under identical experimental conditions. It was clearly revealed that the two studied modified SBA-15 catalysts greatly facilitated the production of SPLs with MCFAs. Besides, the meso-Ph-SO_3H-SBA-15 catalyst with more Brönsted acid sites exhibited the higher reactivities, which could support the aforementioned hypothesis. Furthermore, these results indicated that the strong acidities in the two SBA-15 solid acids and their ordered mesostructure natures as well could improve the accessibility of reactants to the active sites, resulting in the satisfactory catalytic behavior in the SL interesterification reactions [39].

Correspondingly, the results of optimal reaction conditions regarding the meso-Ph-SO_3H-SBA-15 and meso-Pr-SO_3H-SBA-15 catalysts are listed in Figure 6. With respect to the meso-Ph-SO_3H-SBA-15 sample, the influence of reaction time was first assessed by changing the time from 4 to 12 h while keeping all other reaction conditions constant. It is depicted in Figure 6A that the incorporations of MCFAs gradually increased with the reaction time. The maximum values (ca. 15.47 ± 0.53% for C10:0 and ca. 14.25 ± 0.32% for C8:0) were attained at 6 h and significantly declined when the time was further extended. This might be explained by the consequent hydrolysis of SPL products into by-products, which could cover and partially deactivate the surface acid sites [11]. Then the effect of reaction temperature was investigated in the range of 30 °C –70 °C. The results (Figure 6B) clearly showed that about 16.21 ± 0.22% incorporation of C10:0 and around 14.28 ± 0.20% incorporation of C8:0 were obtained at the initial 30 °C. And then the two values were respectively increased to ca. 17.97 ± 0.55% and 16.00 ± 0.37% upon heating to 40 °C. After the reaction temperature was further increased to 70 °C, the incorporations of C10:0 and C8:0 were drastically reduced to about 14.93 ± 0.60% and 12.97 ± 0.21%, almost owing to the decomposition of targeted SPLs into by-products at higher temperatures, as discussed before [12]. In the case of the meso-Pr-SO_3H-SBA-15 catalyst, similar optimized results of the two aforementioned parameters were attained. Therefore, consecutively prolonging the reaction time and/or enhancing the reaction temperature would hardly exhibit any favorable effect on the SL interesterification process.

Thereafter, the influences of mass ratio (SL to methyl caprate or caprylate) and catalyst loading on the SL interesterification over the two functionalized SBA-15 solid acids were also researched and the data are shown in Figure 6C,D. As for the meso-Ph-SO_3H-SBA-15 catalyst, it was clearly seen from Figure 6C that the incorporations of MCFAs progressively increased from ca. 18.97 ± 0.34% to ca. 23.47 ± 0.50% for C10:0 and from ca. 16.00 ± 0.52% to ca. 21.00 ± 0.35% for C8:0 by enhancing the mass ratios from 1:4 to 1:12. This might be ascribed to the fact that higher concentrations of methyl caprate or caprylate in reaction mixtures would promote the formations of targeted SPLs by offering much more acyl groups during the interesterification reactions. Then slight declines of the values were observed when the mass ratios were further increased, which most likely resulted from the deposition of extra methyl caprate or caprylate on the catalyst surfaces and the occupation of the active acid sites [40]. With respect to the effect of catalyst loading, the tests were carried out ranging from 2.5 to 12.5 wt%. According to the results (Figure 6D), it was noticeable that as high as ca. 27.03 ± 0.98% incorporation of C10:0 and ca. 22.21 ± 1.13% of C8:0 were gained when the catalyst loading was 5 wt%. When the parameter was continuously raised up to 12.5 wt%, the two values declined rapidly to around 22.01 ± 0.98% and 18.73 ± 0.66%, respectively. The proposed reason for the

decrease trend could be that the SPLs formed in the SL interesterification were partially converted to by-products [12]. In addition, excess catalyst could make the reaction mixture more viscous and then decrease the effective mass transfer of reactants to active acid sites, which would ultimately result in the reduction of incorporations [40]. Meanwhile, similar changing trends of these two parameters for the meso-Pr-SO_3H-SBA-15 catalyst were attained as well.

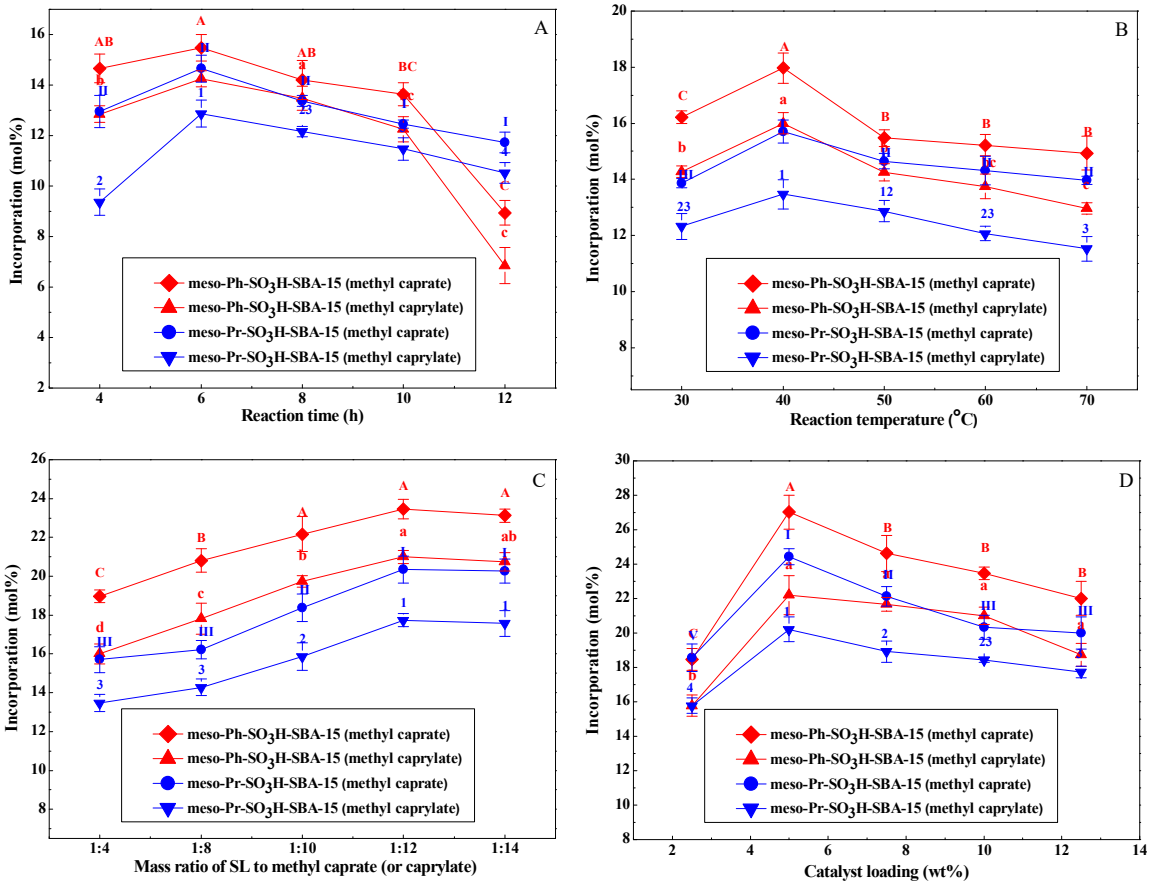

Figure 6. (**A**) Effect of reaction time on SL interesterification over two modified SBA-15 samples. SL: 0.1 g, methyl caprate (or caprylate): 1.45 g (or 1.20 g), catalyst: 10 wt% of total mass, 50 °C. (**B**) Effect of reaction temperature on SL interesterification over two modified SBA-15 samples. SL: 0.1 g, methyl caprate (or caprylate): 1.45 g (or 1.20 g), catalyst: 10 wt% of total mass, 6 h. (**C**) Effect of mass ratio (SL to methyl caprate or caprylate) on SL interesterification over two modified SBA-15 samples. SL: 0.1 g, catalyst: 10 wt% of total mass, 40 °C, 6 h. (**D**) Effect of catalyst loading on SL interesterification over two modified SBA-15 samples. SL: 0.1 g, methyl caprate (or caprylate): 1.45 g (or 1.20 g), 40 °C, 6 h. Values of different groups with different upper-case letters, lower-case letters or numbers are significantly different at $p < 0.05$.

The solvent system is always being regarded as one of the key features of reaction kinetics. It is necessary to optimize this crucial factor so as to achieve satisfactory catalytic activity [5]. Hence, the effect of the solvent system on the catalytic performance of mesoporous organosulfonic acid-modified SBA-15 in SL interesterification was tested in the next step. From the data illustrated in Figure 7A, it could be seen that the two SBA-15 solid acids in hexane exhibited superior MCFA incorporations, meaning that the SL interesterification should be carried out in a hexane solvent system. Simultaneously, the meso-Ph-SO_3H-SBA-15 catalyst showed an exceptional catalytic performance with up to ca. 30.99 ± 0.65% incorporation of C10:0 and ca. 27.03 ± 0.56% of C8:0. Furthermore, it was noted that the MCFA incorporations in non-polar solvent and/or solvent-free systems were much

more than those in polar solvent systems. Generally, non-polar solvent systems were suitable for interesterification, which was attributed to the higher solubility values for substrates in non-polar solvents. Otherwise, the two studied catalysts showed higher activities in the non-polar solvent than in the solvent-free system, mostly because of the viscosity reduction in the reaction mixture caused by non-polar solvent addition and the subsequent enhancement of effective mass transfer [5,41]. Accordingly, the present work should be performed at 40 °C for 6 h with a catalyst loading of 5 wt% in a hexane solvent system for the following studies.

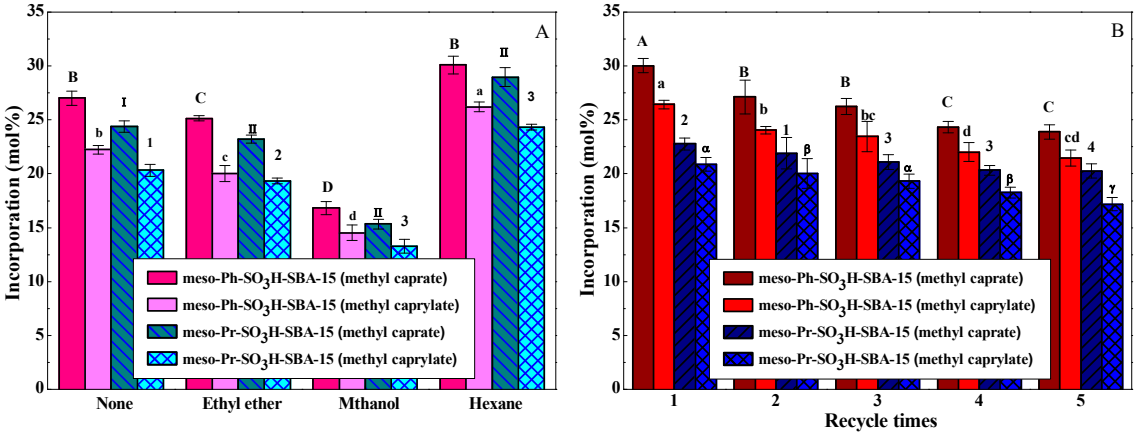

Figure 7. (**A**) Effect of solvent system on SL interesterification over two modified SBA-15 samples. SL: 0.1 g, methyl caprate (or caprylate): 1.45 g (or 1.20 g), catalyst: 0.078 g for methyl caprate or 0.065 g for methyl caprylate, solvent: 5 mL, 40 °C, 6 h. (**B**) Recyclability tests of two modified SBA-15 samples for SL interesterification. SL: 0.1 g, methyl caprate (or caprylate): 1.45 g (or 1.20 g), catalyst: 0.078 g for methyl caprate or 0.065 g for methyl caprylate, hexane: 5 mL, 40 °C, 6 h. Values of different groups with different upper-case letters, lower-case letters, numbers or Greek letters are significantly different at $p < 0.05$.

Under the optimized reaction conditions, the MCFA-enriched SPLs were subsequently produced through SL interesterification by using the above-discussed catalysts. For comparison purposes, the total FA compositions of interesterification products together with SL reactants were quantitatively identified. As summarized in Table 1, FA profiles of the resulting SPL products differed noticeably from those of SL feedstocks. Originally, the FAs found in the SL materials were oleic acid (ca. 66.36 ± 0.46%), linoleic acid (ca. 22.05 ± 0.25%), palmitic acid (ca. 7.39 ± 0.31%) and stearic acid (ca. 4.18 ± 0.53%). After the catalytic interesterification reactions, capric or caprylic acids were detected and their contents were significantly enhanced, revealing that the MCFAs were successfully introduced into the targeted SPLs. Otherwise, the achieved incorporation values were superior to those attained by using expensive phospholipases or lipases at higher temperatures for longer times [11,12]. Thus, it was concluded that the mesoporous sulfonic acid-modified SBA-15 could efficiently catalyze the SL interesterification reactions to produce the MCFA-enriched SPLs under much milder conditions.

Table 1. Total FA composition (mol%) of SLs and SPL products [a].

FA	C8:0	C10:0	C16:0 [c]	C18:0 [c]	C18:1 [c]	C18:2 [c]
SPL (Ph [b])	26.17 ± 0.44	0	6.16 ± 0.12	3.52 ± 1.03	49.43 ± 0.54	14.72 ± 0.23
	0	30.92 ± 0.83	4.99 ± 0.33	2.71 ± 0.74	44.47 ± 0.82	16.91 ± 0.35
SPL (Pr [b])	23.22 ± 0.25	0	6.74 ± 0.27	3.94 ± 0.55	45.36 ± 0.90	20.74 ± 0.41
	0	27.82 ± 0.87	4.58 ± 0.29	3.81 ± 1.01	45.57 ± 0.37	18.22 ± 0.53
SL	0	0	7.39 ± 0.31	4.18 ± 0.53	66.36 ± 0.46	22.05 ± 0.25

[a] Reaction conditions: SL (0.1 g), methyl caprate (1.45 g) or methyl caprylate (1.20 g), catalyst (0.078 g for methyl caprate or 0.065 g for methyl caprylate), hexane (5 mL), 40 °C, 6 h. [b] Ph = meso-Ph-SO_3H-SBA-15 catalyst, Pr = meso-Pr-SO_3H-SBA-15 catalyst. [c] C16:0 = palmitic acid, C18:0 = stearic acid, C18:1 = oleic acid, C18:2 = linoleic acid. Data were reported as mean ± standard deviation.

2.3. Recyclability of the Sulfonic Acid-Modified SBA-15 Catalysts

The catalyst reusability plays a vital role in evaluating its efficiency for industrial application. To achieve this, the stability of the functionalized SBA-15 materials was investigated in the catalytic production of SPLs with MCFAs. The tests were carried out under the optimized experimental conditions for five cycles. After each test run, the used catalyst was centrifuged, respectively washed with diethyl ether and methanol to remove both polar and non-polar compounds adsorbed on the catalyst, and finally vacuum-dried at 80 °C overnight for the next run. As displayed in Figure 7B, no significant changes in MCFA incorporations were observed after five consecutive cycles for each SBA-15 solid acid, suggesting that the two discussed catalysts exhibited long-term cycling stability. In general, with respect to sulfonic acid-modified SBA-15 materials, the losses in catalytic performances were primarily caused by the leaching of sulfur species [42]. Elemental analyses were first performed to determine the product solutions and the results revealed that no obvious leaching of sulfur occurred after the tests. Additionally, the FT-IR spectra of the two reused modified SBA-15 samples are presented in Figure 8A. It was obvious that the characteristic bands ascribed to organosulfonic acid groups remained almost unchanged even after five repeated cycles. Hence, all the aforementioned results indicated that surface-grafted sulfonic acid groups on the studied solid acids were stable under mild conditions. Another hypothesis was proposed that reactants or products might partially occupy the active acid sites, resulting in the pore blockage and slight catalyst deactivation as described in previous publications [14,40]. Therefore, thus-synthesized sulfonic acid-functionalized SBA-15 possessed excellent activity and stability in SL interesterification, which was essential for its potential application in the production of SPLs.

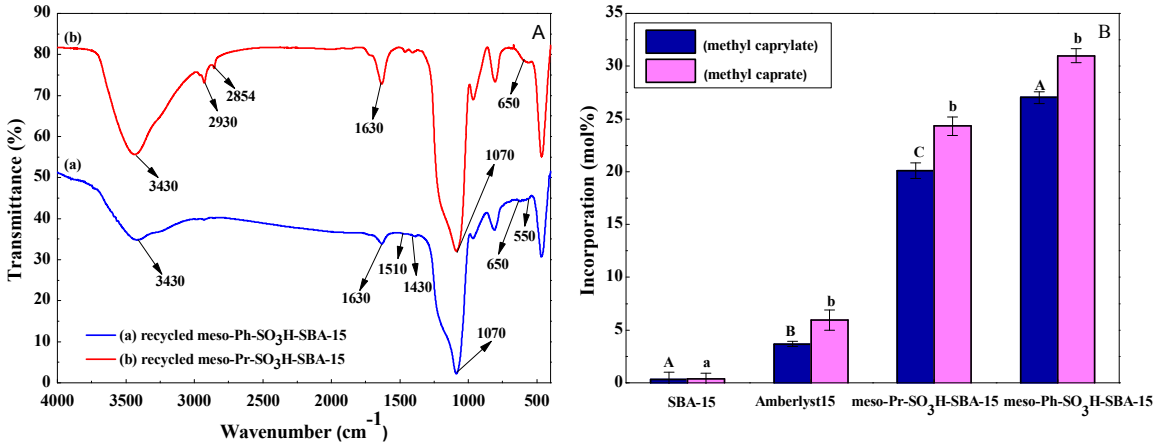

Figure 8. (**A**) FT-IR spectra of two recycled modified SBA-15 samples. (**B**) Comparison of catalytic performances of two modified SBA-15 samples with commercial Amberlyst-15. SL: 0.1 g, methyl caprate (or caprylate): 1.45 g (or 1.20 g), catalyst: 0.078 g for methyl caprate or 0.065 g for methyl caprylate, hexane: 5 mL, 40 °C, 6 h. Values of different groups with different upper-case or lower-case letters are significantly different at $p < 0.05$.

In order to further evaluate the efficiencies of the two SBA-15 type solid acids, their catalytic activities were compared with those of the commercially available Brönsted acid Amberlyst-15 [16] under identical conditions. As depicted in Figure 8B, the incorporations of C10:0 and C8:0 over the meso-Ph-SO_3H-SBA-15 catalyst were up to ca. 30.99 ± 0.65% and 27.03 ± 0.56%, respectively. As for the meso-Pr-SO_3H-SBA-15 catalyst, the two values were as high as ca. 24.32 ± 0.87% and 20.11 ± 0.33%. In contrast, the two incorporation values for Amberlyst-15 drastically declined to ca. 5.95 ± 0.96% and 3.68 ± 0.24%. Thus, it was clearly suggested that the researched SBA-15 catalysts exhibited superior activities in comparison with the typical industrial Amberlyst-15.

3. Materials and Methods

3.1. Materials

Standard fatty acid methyl esters (purity ≥ 99 wt%), poly(ethylene glycol)-block-poly(propylene glycol)-block-ploy(ethylene glycol) (P123, average molecular mass=5800), 3-mercaptopropyltrimethoxysilane (95 wt% purity) and trimethoxyphenylsilane (98 wt% purity) were purchased from Sigma-Aldrich, U.S.A. Soybean lecithin was obtained from Sangon Biotech, China. Methyl caprylate (purity ≥ 99 wt%), methyl caprate (purity ≥ 99 wt%) and tetraethoxysilane (98 wt% purity) were supplied by Aladdin, China. All other chemicals and reagents were of chromatographic or analytical grade and used without further purification.

3.2. Catalyst Preparation

The mesoporous SBA-15 silica was prepared by a hydrothermal method described previously [43]. Briefly, 2.5 g of P123 was dissolved in 75 mL of 1.6 mol/L aqueous hydrochloric acid solution at 40 °C under magnetic stirring. Then, 5.2 g of tetraethoxysilane was added dropwise. Afterwards, the attained mixture was stirred at 40 °C for 24 h, transferred into 100 mL of Teflon-lined stainless steel autoclave and heated at 100 °C for 48 h. Then, the solid sample was collected by filtration, washed with deionized water and dried at 60 °C. Finally, the white solid was calcined at 550 °C for 6 h.

The meso-Pr-SO_3H-SBA-15 was synthesized as reported in the previous literature [33]. Typically, a mixture of SBA-15 (1.0 g) and 3-mercaptopropyltrimethoxysilane (3.0 g) was added into 25 mL of anhydrous toluene, and then the suspension was refluxed under N_2 flow for 30 h. After filtration and thorough washing with diethyl ether, the precipitate was Soxhlet-extracted in a dichloromethane-diethyl ether (1:1, volume ratio) mixture for 10 h and dried in a vacuum oven at 80 °C for 12 h. Subsequently, the obtained solid was oxidized with 30 mL of aqueous H_2O_2 (30 wt%) at 20 °C for 24 h and further acidified with 80 mL of 0.5 M H_2SO_4. The as-prepared catalyst was filtered, washed with deionized water and finally dried at 80 °C under vacuum overnight.

The meso-Ph-SO_3H-SBA-15 was prepared using the following procedures described in the published literature [39]. In a typical run, trimethoxyphenylsilane (3.0 g) was initially suspended in a mixture of SBA-15 (1.0 g) in toluene (20 mL) and refluxed under N_2 atmosphere for 24 h. After the filtration, Soxhlet-extraction in toluene for 10 h and vacuum-drying at 90 °C for 10 h, the formed solid (1.0 g) was added into 30 mL of 1,2-dichloroethane and refluxed under N_2 flow for 2 h. Afterwards, 15 mL of chlorosulfonic acid was added dropwise into the above-mentioned solution, and the resulting mixture was continuously stirred and refluxed under N_2 atmosphere for 6 h. Thereafter, the precipitated solid was separated by filtration and thoroughly washed with ethanol. Finally, the thus-synthesized catalyst could be attained by vacuum-drying at 80 °C for 12 h.

3.3. Catalyst Characterization

XRD measurements were conducted on a Rigaku D/MAX 2400 diffractor (Tokyo, Japan) using Cu Kα radiation at 40 kV and 30 mA. Nitrogen adsorption–desorption isotherms were determined at -193 °C on an ASAP 2010 Micrometrics apparatus (Norcross, GA, U.S.A.). The specific surface area was calculated by the BET method. And the pore-size distribution and total pore volume were evaluated according to the BJH method. SEM was conducted on a JSM-7800F field-emission microscope (JEOL, Tokyo, Japan) equipped with X-Max50 detection (Oxford Instruments, London, U.K.) and operated at 15 kV. TEM images were taken on a JEM-2100 microscope (JEOL, Tokyo, Japan) at 200 kV accelerating voltage.

FT-IR spectra were carried out on a Digilab FTS 3100 spectrometer (Holliston, MA, U.S.A.) using the standard KBr pellet technique in the range of 400–4000 cm^{-1}. FT-IR spectra of pyridine adsorption were recorded on the same instrument based on the procedures reported in our previous literature [30]. The shown spectra were obtained by subtracting the spectra recorded before and after pyridine adsorption. And the ratio of the concentration of strong Brönsted acid sites to Lewis

sites was semi-quantified based on the ratio of the peak areas at around 1546 cm^{-1} and 1446 cm^{-1}, respectively [44,45]. The Brönsted acid site density of the sample was estimated by using 2 M NaCl solution as the exchange agent and 0.01 M NaOH standard solution as the titration agent [46].

3.4. Catalytic Tests

The catalytic interesterification of SL (0.1 g) with methyl caprate or caprylate was tested in a 25 mL of Schlenk tube. Typically, a mixture of SL and powdered catalyst was added into methyl caprate or caprylate. The reactor was then heated to the target temperature (30 °C–70 °C) by magnetic stirring at 700 rpm. Subsequently, the reaction was executed under solvent-free conditions or in an organic solvent system. As for the blank reaction, the mixture of SL (0.1 g) with methyl caprate (1.45 g) or methyl caprylate (1.20 g) was heated at 50 °C for 4 h without adding any catalyst and solvent, and then compared with the results of the catalytic interesterifications to elucidate the critical roles of these SBA-15 type materials.

After the reaction, the reactor was cooled down to room temperature. The reaction mixture was centrifuged to obtain the supernatant liquid, and the precipitate was washed three times with 5 mL of chloroform. Thereafter, the combined chloroform washes were mixed with the supernatant liquid, followed by chloroform evaporation. Then, 5 mL of acetone was added into the resulting lipid mixture, stirred at 4 °C for 1 min and then centrifuged to separate the phospholipid precipitate [47]. The resultant phospholipid pellet was thoroughly washed with another 5 mL of acetone. After the centrifugation and vacuum-drying for 30 min, the pellet sample was finally stored at -40 °C until processing [48]. Additionally, the optimized experimental conditions, such as reaction time, reaction temperature, mass ratio, catalyst loading and solvent system, etc., were systematically explored in order to assess the catalytic activity.

3.5. Analysis of the Fatty Acid Composition

The total FA composition of SLs or interesterification products were determined after converting FA residues in phospholipid samples into the corresponding fatty acid methyl esters (FAMEs) according to the method described by Hartman and Lago [49]. Subsequently, the analyses of the obtained FAMEs were conducted on a Shimadzu Model 2010 Plus gas chromatograph (Kyoto, Japan), fitted with a Shimadzu AOC-20i auto sample injector (Kyoto, Japan), a flame ionization detector and a software package for system control and data acquisition (Shimadzu LabSolutions GC Workstation, version 5.73, Kyoto, Japan). Injections were performed in a fused silica capillary column (30 m*0.25 mm internal diameter) coated with 0.25 μm of Restek Rtx®-5 (Bellefonte, PA, U.S.A.) using nitrogen as the carrier gas at a flow rate of 1.5 mL/min at a split ratio of 1:50. The operating temperatures of the injector and detector were set at 250 °C and 300 °C, respectively. The initial temperature of the oven was set at 160 °C for 3 min, and then programmed to increase to 220 °C at a rate of 5 °C/min, followed by a further increase to 260 °C (30 °C/min) for another 3 min at the final temperature. The injection volume of the FAME sample was 1 μL. The qualitative identification of FA composition was made by comparing the relative retention times of FAME peaks from the sample with those of the respective commercial FAME standards [50]. And the quantitative FA composition was obtained by an external standard method and expressed as a molar percentage. The relative amounts of FAs in the phospholipid sample were calculated according to the response factors of the FAME standards in units of mol%. Moreover, the catalytic performances of the studied materials on the SL interesterification were evaluated by the relative amounts of MCFAs from SPLs in the form of incorporations. And these MCFA incorporations were determined as the molar percentages of capric or caprylic acids introduced into the SPL products. All determinations of the FAME sample were done in triplicate and the values reported in this work were averaged over three runs [47].

3.6. Statistical Analysis

All of the interesterification reactions were conducted in triplicate. The statistical analysis was performed by using SPSS 22.0 software (Chicago, IL, U.S.A.). The data were presented as mean ± standard deviation based on our previous method [30]. A P value < 0.05 was considered statistically significant.

4. Conclusions

This work thoroughly studied the production of medium-chain SPLs by SL interesterification over two mesoporous organosulfonic acid-functionalized SBA-15 catalysts. It was proposed that the MCFA incorporations were greatly influenced by the acidic properties and mesoporous structures of the catalysts. In contrast to Lewis acid sites, the adequate Brönsted acid sites on the surfaces of catalysts were more conducive to SPL production. Besides, the ordered mesostructures of the SBA-15 type catalysts could improve the accessibilities of SL feedstocks. Hence, under the optimum conditions of 40 °C and 6 h, the maximum incorporations of C10:0 and C8:0, respectively, reached up to around 30.99 ± 0.65% and 27.03 ± 0.56% by using the meso-Ph-SO_3H-SBA-15 catalyst. Meanwhile, the two values for the meso-Pr-SO_3H-SBA-15 catalyst were about 24.32 ± 0.87% and 20.11 ± 0.33%. Otherwise, the two functionalized SBA-15 catalysts could be repeatedly used without significant loss in reaction activity during five consecutive tests. When further compared with the commercial Amberlyst-15, the two catalysts demonstrated much better catalytic performances. Therefore, the positive results in this work might shed light on the development of efficient, economical and eco-friendly catalysts for the production of MCFA-enriched SPLs in a heterogeneous manner, achieving the goal of producing high-valued chemicals, pharmaceuticals and nutraceuticals from natural lipids.

Author Contributions: Conceptualization and proposed methodology, J.Z., D.Z. and B.Z.; investigation, J.Z., S.Y. and J.J.; writing—original draft, J.Z., S.Y. and J.J.; writing—review and editing, D.Z., W.C. and F.Y.

Funding: This research was funded by the National Natural Science Foundation of China (Grant No. 31801546), China Postdoctoral Science Foundation Funded Project (Grant No. 2017M621119), Key Programs of Natural Science Foundation of Liaoning Province (Grant No. 20170520220), Project of Distinguished Professor of Liaoning Province (Grant No. 2015-153) and National Key R&D Program of China (Grant No. 2017YFB0308701).

Acknowledgments: The authors are grateful for the financial support from the National Natural Science Foundation of China (Grant No. 31801546), China Postdoctoral Science Foundation Funded Project (Grant No. 2017M621119), Key Programs of Natural Science Foundation of Liaoning Province (Grant No. 20170520220), Project of Distinguished Professor of Liaoning Province (Grant No. 2015-153) and National Key R&D Program of China (Grant No. 2017YFB0308701).

Conflicts of Interest: The authors declare no conflict of interest.

References

1. Xie, W.; Chen, J. Heterogeneous interesterification of triacylglycerols catalyzed by using potassium-doped alumina as a solid catalyst. *J. Agric. Food Chem.* **2014**, *62*, 10414–10421. [CrossRef] [PubMed]
2. Sivakanthan, S.; Jayasooriya, A.P.; Madhujith, T. Optimization of the production of structured lipid by enzymatic interesterification from coconut (*Cocos nucifera*) oil and sesame (*Sesamum indicum*) oil using Response Surface Methodology. *LWT-Food Sci. Technol.* **2019**, *101*, 723–730. [CrossRef]
3. Xie, W.; Hu, P. Production of structured lipids containing medium-chain fatty acids by soybean oil acidolysis using SBA-15-pr-NH_2-HPW catalyst in a heterogeneous manner. *Org. Process Res. Dev.* **2016**, *20*, 637–645. [CrossRef]
4. Wang, X.; Zou, S.; Miu, Z.; Jin, Q.; Wang, X. Enzymatic preparation of structured triacylglycerols with arachidonic and palmitic acids at the sn-2 position for infant formula use. *Food Chem.* **2019**, *283*, 331–337. [CrossRef] [PubMed]
5. Kim, J.H.; Yoon, S.H. Effects of organic solvents on transesterification of phospholipids using phospholipase A_2 and lipase. *Food Sci. Biotechnol.* **2014**, *23*, 1207–1211. [CrossRef]
6. Reddy, J.R.C.; Vijeeta, T.; Karuna, M.S.L.; Rao, B.V.S.K.; Prasad, R.B.N. Lipase-catalyzed preparation of palmitic and stearic acid-rich phosphatidylcholine. *J. Am. Oil Chem. Soc.* **2005**, *82*, 727–730. [CrossRef]

7. Lee, H.S.; Sung, D.K.; Kim, S.H.; Choi, W.I.; Hwang, E.T.; Choi, D.J.; Chang, J.H. Controlled release of astaxanthin from nanoporous silicified-phospholipids assembled boron nitride complex for cosmetic applications. *Appl. Surf. Sci.* **2017**, *424*, 15–19. [CrossRef]
8. Kim, B.H.; Akoh, C.C. Recent research trends on the enzymatic synthesis of structured lipids. *J. Food Sci.* **2015**, *80*, C1713–C1724. [CrossRef]
9. Lemaitre-Delaunay, D.; Pachiaudi, C.; Laville, M.; Pousin, J.; Armstrong, M.; Lagarde, M. Blood compartmental metabolism of docosahexaenoic acid (DHA) in humans after ingestion of a single dose of [^{13}C]DHA in phosphatidylcholine. *J. Lipid Res.* **1999**, *40*, 1867–1874.
10. Chojnacka, A.; Gładkowski, W.; Gliszczyńska, A.; Niezgoda, N.; Kiełbowicz, G.; Wawrzeńczyk, C. Synthesis of structured phosphatidylcholine containing punicic acid by the lipase-catalyzed transesterification with pomegranate seed oil. *Catal. Commun.* **2016**, *75*, 60–64. [CrossRef]
11. Zhao, T.T.; No, D.S.; Kim, B.H.; Garcia, H.S.; Kim, Y.; Kim, I.H. Immobilized phospholipase A1-catalyzed modification of phosphatidylcholine with n-3 polyunsaturated fatty acid. *Food Chem.* **2014**, *157*, 132–140. [CrossRef] [PubMed]
12. Ochoa, A.A.; Hernández-Becerra, J.A.; Cavazos-Garduño, A.; García, H.S.; Vernon-Carter, E.J. Phosphatidylcholine enrichment with medium chain fatty acids by immobilized phospholipase A_1-catalyzed acidolysis. *Biotechnol. Progr.* **2013**, *29*, 230–236. [CrossRef] [PubMed]
13. Akinfalabi, S.I.; Rashid, U.; Choong Shean, T.Y.; Nehdi, I.A.; Sbihi, H.M.; Gewik, M.M. Esterification of palm fatty acid distillate for biodiesel production catalyzed by synthesized kenaf seed cake-based sulfonated catalyst. *Catalysts* **2019**, *9*, 482. [CrossRef]
14. Gaidukevic, J.; Barkauskas, J.; Malaika, A.; Rechnia-Goracy, P.; Mozdzynska, A.; Jasulaitiene, V.; Kozlowski, M. Modified graphene-based materials as effective catalysts for transesterification of rapeseed oil to biodiesel fuel. *Chin. J. Catal.* **2018**, *39*, 1633–1645. [CrossRef]
15. Fu, X.; Li, D.; Chen, J.; Zhang, Y.; Huang, W.; Zhu, Y.; Yang, J.; Zhang, C. A microalgae residue based carbon solid acid catalyst for biodiesel production. *Bioresource Technol.* **2013**, *146*, 767–770. [CrossRef] [PubMed]
16. Di Serio, M.; Tesser, R.; Pengmei, L.; Santacesaria, E. Heterogeneous catalysts for biodiesel production. *Energy Fuel* **2008**, *22*, 207–217. [CrossRef]
17. Garcia, C.M.; Teixeira, S.; Marciniuk, L.L.; Schuchardt, U. Transesterification of soybean oil catalyzed by sulfated zirconia. *Bioresource Technol.* **2008**, *99*, 6608–6613. [CrossRef] [PubMed]
18. Kobayashi, H.; Ito, S.; Hara, K.; Fukuoka, A. Conversion of glycerol to acrolein by mesoporous sulfated zirconia-silica catalyst. *Chin. J. Catal.* **2017**, *38*, 420–425. [CrossRef]
19. Zhang, P.; Wu, H.; Fan, M.; Sun, W.; Jiang, P.; Dong, Y. Direct and postsynthesis of tin-incorporated SBA-15 functionalized with sulfonic acid for efficient biodiesel production. *Fuel* **2019**, *235*, 426–432. [CrossRef]
20. Zuo, D.; Lane, J.; Culy, D.; Schultz, M.; Pullar, A.; Waxman, M. Sulfonic acid functionalized mesoporous SBA-15 catalysts for biodiesel production. *Appl. Catal. B-Environ.* **2013**, *129*, 342–350. [CrossRef]
21. Gardy, J.; Hassanpour, A.; Lai, X.; Ahmed, M.H. Synthesis of Ti(SO_4)O solid acid nano-catalyst and its application for biodiesel production from used cooking oil. *Appl. Catal. A-Gen.* **2016**, *527*, 81–95. [CrossRef]
22. Cattaneo, A.S.; Ferrara, C.; Villa, D.C.; Angioni, S.; Milanese, C.; Capsoni, D.; Grandi, S.; Mustarelli, P.; Allodi, V.; Mariotto, G.; et al. SBA-15 mesoporous silica highly functionalized with propylsulfonic pendants: A thorough physico-chemical characterization. *Microporous Mesoporous Mater.* **2016**, *219*, 219–229. [CrossRef]
23. Jin, H.; Ansari, M.B.; Park, S. Sulfonic acid functionalized mesoporous ZSM-5: Synthesis, characterization and catalytic activity in acidic catalysis. *Catal. Today* **2015**, *245*, 116–121. [CrossRef]
24. Sing, K.S.W.; Everett, D.H.; Haul, R.A.W.; Moscou, L.; Pierotti, R.A.; Rouquerol, J.; Siemieniewska, T. Reporting physisorption data for gas/solid systems with special reference to the determination of surface area and porosity. *Pure Appl. Chem.* **1985**, *57*, 603–619. [CrossRef]
25. Chu, Q.; Chen, J.; Hou, W.; Yu, H.; Wang, P.; Liu, R.; Song, G.; Zhu, H.; Zhao, P. Enhancement of catalytic activity by homo-dispersing $S_2O_8^{2-}$-Fe_2O_3 nanoparticles on SBA-15 through ultrasonic adsorption. *Chin. J. Catal.* **2018**, *39*, 955–963. [CrossRef]
26. Srivastava, R. An efficient, eco-friendly process for aldol and Michael reactions of trimethylsilyl enolate over organic base-functionalized SBA-15 catalysts. *J. Mol. Catal. A-Chem.* **2007**, *264*, 146–152. [CrossRef]
27. Isaacs, M.A.; Robinson, N.; Barbero, B.; Durndell, L.J.; Manayil, J.C.; Parlett, C.M.A.; D'Agostino, C.; Wilson, K.; Lee, A.F. Unravelling mass transport in hierarchically porous catalysts. *J. Mater. Chem. A* **2019**, *7*, 11814–11825. [CrossRef]

28. Zhao, D.; Feng, J.; Huo, Q.; Melosh, N.; Fredrickson, G.H.; Chmelka, B.F.; Stucky, G.D. Triblock copolymer syntheses of mesoporous silica with periodic 50 to 300 angstrom pores. *Science* **1998**, *279*, 548–552. [CrossRef]
29. Lin, C.; Tao, K.; Yu, H.; Hua, D.; Zhou, S. Enhanced catalytic performance of molybdenum-doped mesoporous SBA-15 for metathesis of 1-butene and ethene to propene. *Catal. Sci. Technol.* **2014**, *4*, 4010–4019. [CrossRef]
30. Zhang, J.; Yang, S.; Zhang, Z.; Cui, L.; Jia, J.; Zhou, D.; Zhu, B. An excellent solid acid catalyst derived from microalgae residue for fructose dehydration into 5-hydroxymethylfurural. *ChemistrySelect* **2019**, *4*, 1259–1265. [CrossRef]
31. Amoozadeh, A.; Rahmani, S. Nano-WO_3-supported sulfonic acid: New, efficient and high reusable heterogeneous nano catalyst. *J. Mol. Catal. A-Chem.* **2015**, *396*, 96–107. [CrossRef]
32. Geng, L.; Wang, Y.; Yu, G.; Zhu, Y. Efficient carbon-based solid acid catalysts for the esterification of oleic acid. *Catal. Commun.* **2011**, *13*, 26–30. [CrossRef]
33. Wang, L.; Zhang, L.; Li, H.; Ma, Y.; Zhang, R. High selective production of 5-hydroxymethylfurfural from fructose by sulfonic acid functionalized SBA-15 catalyst. *Compos. Part B-Eng.* **2019**, *156*, 88–94. [CrossRef]
34. Veisi, H.; Sedrpoushan, A.; Faraji, A.R.; Heydari, M.; Hemmati, S.; Fatahi, B. A mesoporous SBA-15 silica catalyst functionalized with phenylsulfonic acid groups (SBA-15-Ph-SO_3H) as a novel hydrophobic nanoreactor solid acid catalyst for a one-pot three-component synthesis of 2*H*-indazolo[2,1-*b*]phthalazine-triones and triazolo[1,2-*a*]indazole-triones. *RSC Adv.* **2015**, *5*, 68523–68530. [CrossRef]
35. Thapa, I.; Mullen, B.; Saleem, A.; Leibig, C.; Baker, R.T.; Giorgi, J.B. Efficient green catalysis for the conversion of fructose to levulinic acid. *Appl. Catal. A-Gen.* **2017**, *539*, 70–79. [CrossRef]
36. Rao, G.S.; Rajan, N.P.; Sekhar, M.H.; Ammaji, S.; Chary, K.V.R. Porous zirconium phosphate supported tungsten oxide solid acid catalysts for the vapour phase dehydration of glycerol. *J. Mol. Catal. A-Chem.* **2014**, *395*, 486–493. [CrossRef]
37. Chen, F.R.; Coudurier, G.; Joly, J.F.; Vedrine, J.C. Superacid and catalytic properties of sulfated zirconia. *J. Catal.* **1993**, *143*, 616–626. [CrossRef]
38. Morterra, C.; Cerrato, G.; Emanuel, C.; Bolis, V. On the surface acidity of some sulfate-doped ZrO_2 catalysts. *J. Catal.* **1993**, *142*, 349–367. [CrossRef]
39. Miao, S.; Shanks, B.H. Esterification of biomass pyrolysis model acids over sulfonic acid-functionalized mesoporous silicas. *Appl. Catal. A-Gen.* **2009**, *359*, 113–120. [CrossRef]
40. Xie, W.; Zhang, C. Production of medium-chain structured lipids using dual acidic ionic liquids supported on Fe_3O_4@SiO_2 composites as magnetically recyclable catalysts. *LWT Food Sci. Technol.* **2018**, *93*, 71–78. [CrossRef]
41. Li, Z.; Ward, O.P. Lipase-catalyzed esterification of glycerol and n-3 polyunsaturated fatty acid concentrate in organic solvent. *J. Am. Oil Chem. Soc.* **1993**, *70*, 745–748. [CrossRef]
42. Ma, H.; Li, J.; Liu, W.; Cheng, B.; Cao, X.; Mao, J.; Zhu, S. Hydrothermal preparation and characterization of novel corncob-derived solid acid catalysts. *J. Agric. Food Chem.* **2014**, *62*, 5345–5353. [CrossRef] [PubMed]
43. Wang, Y.; Wang, D.; Tan, M.; Jiang, B.; Zheng, J.; Tsubaki, N.; Wu, M. Monodispersed hollow SO_3H-functionalized carbon/silica as efficient solid acid catalyst for esterification of oleic acid. *ACS Appl. Mater. Int.* **2015**, *7*, 26767–26775. [CrossRef] [PubMed]
44. Rocha, A.S.; Forrester, A.M.S.; de la Cruz, M.H.C.; da Silva, C.T.; Lachter, E.R. Comparative performance of niobium phosphates in liquid phase anisole benzylation with benzyl alcohol. *Catal. Commun.* **2008**, *9*, 1959–1965. [CrossRef]
45. Emeis, C.A. Determination of integrated molar extinction coefficients for infrared absorption bands of pyridine adsorbed on solid acid catalysts. *J. Catal.* **1993**, *141*, 347–354. [CrossRef]
46. Margolese, D.; Melero, J.A.; Christiansen, S.C.; Chmelka, B.F.; Stucky, G.D. Direct syntheses of ordered SBA-15 mesoporous silica containing sulfonic acid groups. *Chem. Mater.* **2000**, *12*, 2448–2459. [CrossRef]
47. Marsaoui, N.; Laplante, S.; Raies, A.; Naghmouchi, K. Incorporation of omega-3 polyunsaturated fatty acids into soybean lecithin: Effect of amines and divalent cations on transesterification by lipases. *World J. Microbiol. Biotechnol.* **2013**, *29*, 2233–2238. [CrossRef]
48. Kaki, S.S.; Balakrishna, M.; Prasad, R.B.N. Enzymatic synthesis and characterization of 1-lipoyl-2-palmitoyl phosphatidylcholine: A novel phospholipid containing lipoic acid. *Eur. J. Lipid Sci. Technol.* **2014**, *116*, 1347–1353. [CrossRef]

49. Hartman, L.; Lago, R.C. Rapid preparation of fatty acid methyl esters from lipids. *Lab. Pr.* **1973**, *22*, 475–476.
50. De Martini Soares, F.A.S.; da Silva, R.C.; da Silva, K.C.G.; Lourenço, M.B.; Soares, D.F.; Gioielli, L.A. Effects of chemical interesterification on physicochemical properties of blends of palm stearin and palm olein. *Food Res. Int.* **2009**, *42*, 1287–1294. [CrossRef]